Journal of ELECTRICAL ENGINEERING, VOL 74(2023), NO1, 1–12

sciendo

PAPERS

A new full-duplex analog RoF transmission system for 5G/5G+ broadband mobile communication

Anes Belkacem*, Ahmed Riad Borsali[1]

A new cost-effective mobile fronthaul architecture has been proposed by designing promising analog radio over fiber (ARoF) transmission system compliant with the next generation ultra-dense wavelength division multiplexing passive optical network (UDWDM-PON). It is conceived for standalone 5G/5G+ mobile communication systems driven by broadband multi-input multi-output (MIMO) millimeter wave data signals using two high spectral efficient modulations. The feasibility of the proposed system was firstly proven in terms of spectral tracing supported by theoretical analysis that disclosed good agreement. Furthermore, the obtained simulation results regarding the system performance evaluation after 22 km bidirectional optical fiber links were revealed high reliable characteristics including error-free transmissions at low receiver sensitivities, and measured power penalties less than 1 dB. In addition, the recovered eye diagrams maintained wide openings with high-quality patterns.

K e y w o r d s: analog radio over fiber, UDWDM-PON, millimeter wave, optical flat comb generator, optical polarization multiplexing, mobile fronthaul, MIMO

1 Introduction

The current mobile communication systems are very challenged due to the continuous bandwidth demands of the new multimedia applications that forcing the provision of broadband multi-gigabit per second data connections anytime and anywhere. A modern mobile communication system called fifth-generation 5G new radio (NR) has been evolved by including for the first-time millimeter-wave (mm-mave) bands ranging from 24 GHz to 300 GHz for use [1]. It is reserved to run various enhanced mobile broadband (eMBB) services such as augmented reality (AR), virtual reality (VR), autonomous driving vehicles, ubiquitous cloud computing and real-time video streaming etc. Thereby, to support massive eMBB services in 5G and beyond; it is envisioned to deploy thousands of base stations (BSs) approximately of $40-50\,\mathrm{BSs/km^2}$, [2]. As a result, each BS will be equipped by high frequency electronic local oscillator (ELO). This proceeding is foreseen to be not a future proof solution owing to the fact that the phase noise is directly proportional to the increased frequency [3].

With the standardization endeavors towards robust 5G transport architecture, analog RoF (ARoF) ruled by photonic mm-wave generation techniques is the best rival. It is fully aligned with the next era of centralized radio access network (C-RAN) technology based on passive optical network (PON) [4]. Various photonic mm-wave generation methods have been reported to be applicable for 5G and beyond [5]. Unfortunately, these techniques are suffering from increase in transmitter design complexity, and poor frequency tunability. Moreover, all of them are facing major challenges for massive small cells deployment due to the use of plenty discrete laser sources dependent to the number of installed base stations.

Ultra-dense wavelength division multiplexing (UDWDM) PON has been regarded as an unrivaled competitor that would be devoted to accommodate a large number of small cells in ultra-dense networks (UDNs) [6]. It is becoming an utmost importance of being use a centralized optical multiwavelength generator emits multiple optical carriers by keeping into account the realization of continuous tunable mm-waves generation with low-cost system implementation. Recently, the use of optical frequency comb source (OFCS) has been proven its good proficiency as a favorable solution. It has a paramount intrinsic superiority in terms of which only one laser source is used for generating many optical carriers. Furthermore, low-phase noise mm-waves can be easily generated due to the inherent coherency between the generated optical carriers that issued from the same laser source. In this context, various models were proposed [7-11], but they are subjected to stringent design considerations such complex generator structures, and generating few optical carriers with lacks of flatness. In contrast, flat comb source with broader optical sideband carriers is the feasible solution. It is capable to facilitate spectral resource allocations seamlessly and dynamically. On one hand, in downlink for data transmission, and for remote delivery of unmodulated carriers to be used as beat sources for mm-wave generation at each base station. While on the other hand, leads to simplify the BS architecture by making it laser-

[1] STIC Laboratory, Department of Telecommunication, Faculty of Technology, Abou Bekr Belkaid University, Tlemcen, Algeria, * corresponding author anesbelkacem01@gmail.com

https://doi.org/10.2478/jee-2023-0001, Print (till 2015) ISSN 1335-3632, On-line ISSN 1339-309X

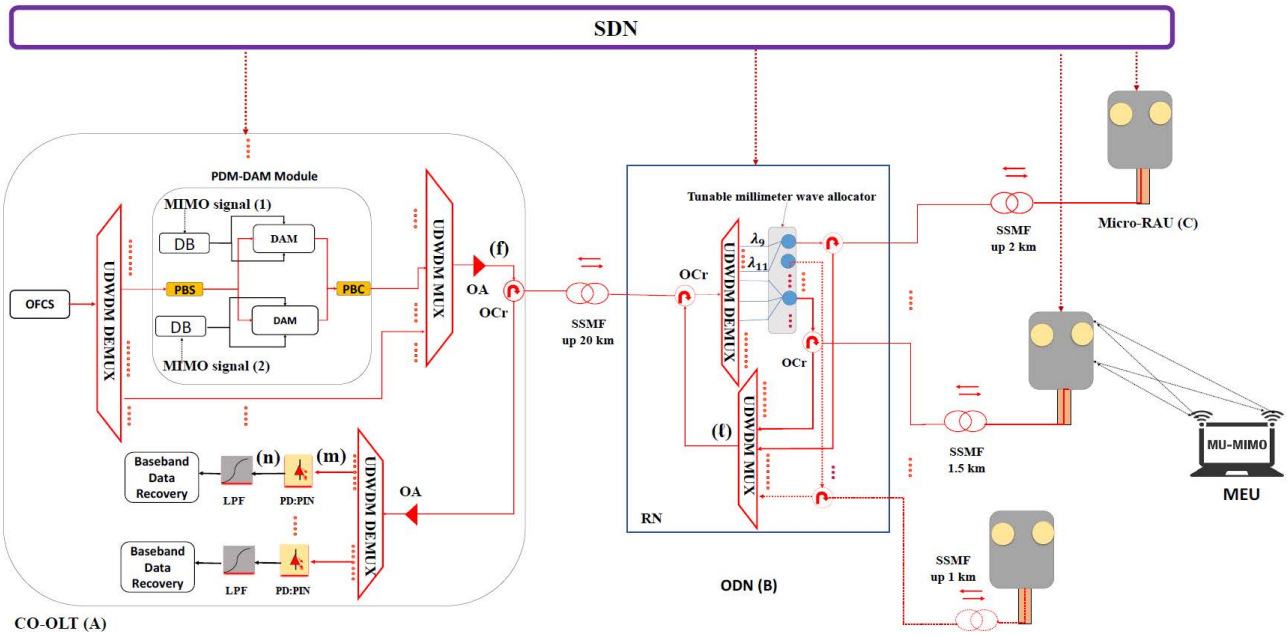

Fig. 1. A complete view of the proposed full-duplex ARoF-PON system

free by reusing those unmodulated carriers for uplink due to its robustness (flat carriers).

To strengthen even further the future 5G/5G+ network capacity requirements, multiple-input multiple-output(MIMO)wireless signals with the incorporation of high spectral efficient data modulations is indispensable ought to be adhered. It is better to determine a data modulation format that can optimally merge some merits of both binary baseband and vector modulation schemes. Multilevel modulation based on ternary signaling termed correlative duobinary coding had revealed interesting virtues, to name a few, efficient bandwidth utilization, small timing jitter, and slight amplitude distortion [12]. It could be also considered as a proper strategy to combat the inherent detrimental effects that deteriorates the analog optical link transmission quality including chromatic dispersion and fiber nonlinearities in dense wavelength division multiplexing transmission systems [13].

Although the concept of duobinary modulation is already proposed in several mm-wave ARoF communication systems [14-16]. Only unidirectional single channel transmission with fixed mm-wave modulated carrier generation methods without considering MIMO technology were demonstrated. In this paper, we suggest a new low-cost and high spectral efficient full-duplex ARoF fronthaul system to transport broadband wireless MIMO signals dedicated for 5G/5G+ mobile communication.

2 Principle work of the proposed full-duplex ARoF-PON system

The proposed ARoF design is a fully centralized mobile fronthaul transport network composed of three major entities which are: central office (CO), optical distribution network (ODN) and multiple micro radio access units (RAUs) installed at small cell sites to serve mobile end users (MEUs) as detailed in Fig. 1.

As shown in Fig. 1, CO houses the optical line terminal (OLT) module where all the major processing tasks such as optical comb lines generation, user data modulation, and optical amplifications are concentrated. In the OLT, multiple coherent optical carriers are generated from an optical flat comb source (OFCS). Once the comb source generates flat optical carriers are introduced to the optical demultiplexer (DEMUX) to be segregated into independent wavelengths. The segregated optical carriers can be tuned continuously to involve data modulation or not via altering the wavelength switching state regulated via the software defined networking (SDN) controller. In the proposed approach, the obtained optical flat carriers after segregation are equally allocated to be used. In downlink, broadband wireless MIMO signals are optically multiplexed over two orthogonal polarization states per carrier by the use of polarization division multiplexing (PDM) technique. On the other hand, the remaining optical carriers are kept unmodulated to be served as beat sources in each base station for millimeter wave generation via remote heterodyne detection (RHD), as well as being re-utilized immediately as carriers to empower wavelength reuse operation for uplink data transmission. The modulated and unmodulated optical signals are multiplexed using UDWDM multiplexer. After that, the multiplexed signals are launched to the remote node (RN) after suitable optical amplification through an optical distribution network (ODN) using feeder standard single mode fiber (SSMF). The RN demultiplexes the downstream optical signals to multiple separated modulated and unmodulated signals. A mm-wave allocator with tunable capability is included. It is used to select the target optical sidebands by coupling at least one modulated carrier with

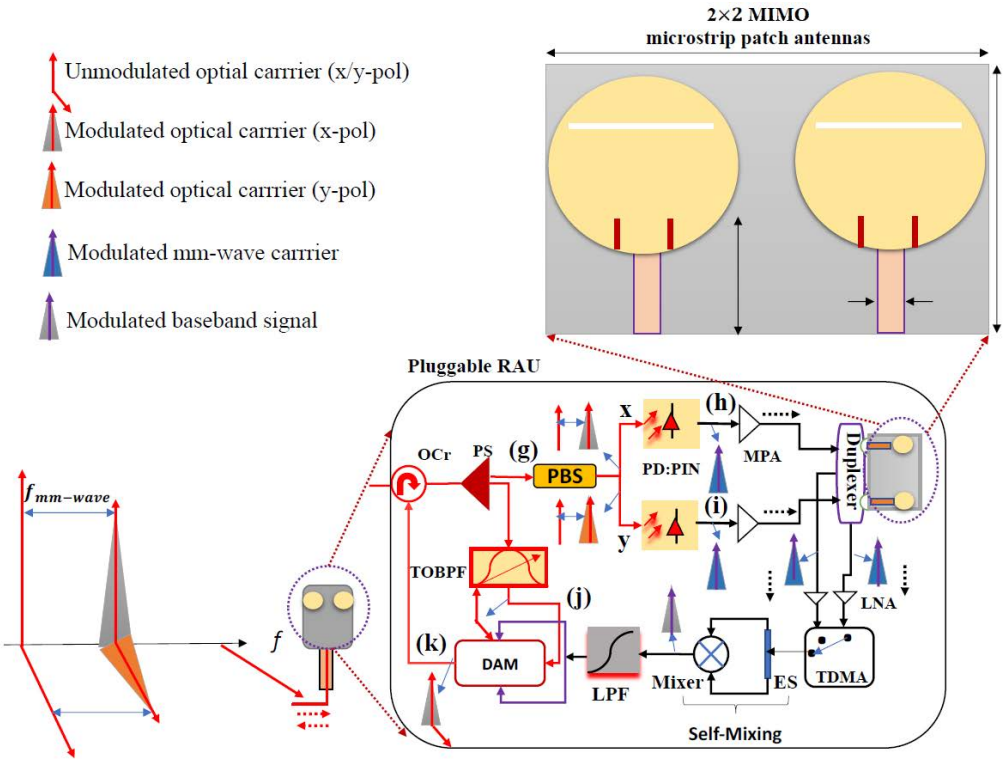

Fig. 2. The proposed new micro-RAU

an arbitrary unmodulated carrier (acts as local oscillator) assigned independently per each remote RAU. It should take into account the frequency spacing between them in order to yield the desired mm-wave band at the RAU by utilizing RHD in accordance to the desired usage scenario for wireless transmission. As a result, this new method is very simple, cost-effective, and offering straightforward continuous tunable mm-wave generation at different frequencies in comparison to the methods used in [5].

After being dynamically allocated, each pair of optically coupled signals carried with same or different frequency spacing are forwarded separately towards their corresponding micro-RAUs over distributed SSMF links. During the whole ODN, neither optical power amplification nor chromatic dispersion compensation are used, and thus, contributing to reduce the deployment cost significantly. Subsequently, the optical coupled signals are received at their RAUs where are given as input to 1×2 power splitters (PSs) to be optically split into two as shown in Fig. 2. At the upper branch (g), the optical modulated and unmodulated signals are polarized demultiplexed into their x and y orthogonal polarization states by means of power beam splitter (PBS) to generate mm-wave signals by beating high-speed photodiodes (PDs). Accordingly, the obtained modulated mm-wave signals are sent out to the mobile end user (MEU) after electrical amplifications through 2×2 MIMO microstrip patch antennas [17] that connected to a compact duplexer in monolithic manner used to allow bidirectional wireless transmission with high isolation.

In uplink direction, the mm-wave MIMO signals travers multipath wireless channel from the MEU to the RAU. At the RAU, the captured data signals are processed by incorporating minimum signal processing and colorless operation before transmission toward the CO as shown in the lower branch of Fig. 2. The process starts by conducting time division multiple access (TDMA) between different mm-wave MIMO signals coming from the duplexer. Then, time multiplexed baseband duobinary signals would be obtained after self-mixing technique. Thereafter, by using the second output of the power splitter, each RAU chooses its intended designated unmodulated optical carrier via a tunable optical band pass filter (TOBPF) by means of SDN controller decision. As a result, colorless operation is realized by making the RAU free from additional laser source. Eventually, the abstracted unmodulated carrier will be intensity modulated by the time multiplexed duobinary baseband signal through a dual-arm Mach Zehnder Modulator (DAM). Likewise, the modulated uplink optical signals from each RAU are transmitted in the opposite direction to the RN to be multiplexed via UDWDM multiplexer (MUX). Thereby, the composite signals are transmitted afterward through the same feeder SMF link toward the CO. At the CO, before demultiplexing; the combined uplink signals are amplified using an optical amplifier (OA) to compensate the power losses. After being divided into N paths via UDWDM DEMUX, are directly detected using array of simple low-frequency photo-detectors (PDs) followed by low pass filters (LPFs) in order to recover the users data from the optical modulated carriers, see Fig. 1.

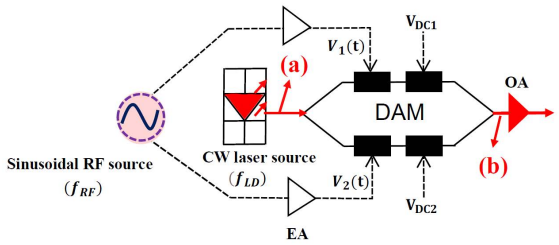

Fig. 3. The schematic diagram of the proposed OFCS

3 System spectral analysis and setup specifications

To confirm the feasibility of the proposed architecture design, an appropriate numerical simulation using professional licensed industrial software named OptiSystem version 18 was carried out according to Fig. 1 and Fig. 2.

The schematic structure of the optical flat comb source (OFCS) shown at the left side of Fig. 1 is detailed in Fig. 3. It simply composed of a continuous wavelength distributed feed-back laser diode (CW DFB-LD), a sinusoidal RF source, pair of electrical power amplifiers (EAs), a dual-arm lithium niobate (LiNbO3) Mach Zehnder Modulator (DAM), and an optical amplifier (OA) to boost the generated optical carriers power. In our setup, CW optical carrier of 193.1 THz is modulated by the RF sinusoidal signal through DAM. The RF signal generator has a pulse repetition frequency rate of 12.5 GHz to conform the International Telecommunication Union (ITU) frequency flex grid with respect to the UDWDM-PON.

Now, through a simple mathematical model, the intrinsic idea that best describes the working principle of the adopted OFC source is presented. The RF sinusoidal wave is split into two sinusoidal RF signals that are electrically amplified to modulate both DAM arms simultaneously. By assuming an equal power division between the upper and lower interferometer DAM arms, the modulated optical field at the DAM output in complex representation is

$$E_{\mathrm{DAM}}(t) = \frac{\alpha E_{\mathrm{LD}}(t)}{2}\Big[\exp\big(j\pi\frac{v_1(t)}{V_\pi}\big)+\exp\big(j\pi\frac{v_2(t)}{V_\pi}\big)\Big], \tag{1}$$

where $\alpha = 10^{-L_{\mathrm{I}}/20}$, L_{I} being is the insertion loss of the DAM modulator. V_π is the required driving half-wave voltage to produce a phase shift of 180°. $E_{\mathrm{LD}}(t)$ denotes the input optical field to the DAM generated from the laser diode (LD),

$$E_{\mathrm{LD}}(t) = \sqrt{P_{\mathrm{LD}}}\exp\big(j\omega_{\mathrm{LD}}t\big), \tag{2}$$

where P_{LD} and f_{LD} indicate the power and center frequency of the optical carrier, respectively using notation $\omega_{\mathrm{LD}} = 2\pi f_{\mathrm{LD}}$. The input optical carrier through the DAM arms is modulated by DC biases shifted effective RF sinusoidal voltages $V_1(t)$ and $V_2(t)$ are

$$v_i(t) = \frac{1}{2}\big(V_{\mathrm{RF}i}\sin\omega_{\mathrm{RF}} + V_{\mathrm{DC}i}\big), \tag{3}$$

where $V_{\mathrm{RF}i}$, $V_{\mathrm{DC}i}$, $(i = 1, 2)$ represent the peak-to-peak RF and the DC bias voltages applied to the DAM arms, respectively, at the RF signal frequency f_{RF}.

In this work, to generate numerous comb lines with good flatness, the DAM should operates in asymmetric mode [18]. In this case, the DC biases voltages are set to be constant ($V_{\mathrm{DC1}} = V_{\mathrm{DC2}} = V_{\mathrm{DC}}$), and different voltages $V_{\mathrm{RF}i}, (i = 1, 2)$ are applied in both DAM arms, denoting: $V_{\mathrm{RF2}} = \kappa V_{\mathrm{RF1}}$

Based on Jacobi-Anger expansion

$$\exp(jm\sin x) = \sum_{n=-\infty}^{\infty} J_n(m)\exp(jnx),$$

where $J_n(.)$ is the n-th order Bessel function of the first kind. The final expression is then obtained as

$$\begin{aligned} E_{\mathrm{DAM}}(t) = {} & \alpha\frac{\sqrt{P_{\mathrm{LD}}}}{2}\exp\big(j\pi\frac{V_{\mathrm{DC}}}{2V_\pi}\big)\times \\ & \sum_{n=-\infty}^{\infty}\left[J_n(\pi\frac{V_{\mathrm{RF1}}}{2V_\pi}) + J_n(\pi\frac{V_{\mathrm{RF2}}}{2V_\pi})\right]\times \cdot \\ & \times\exp\big(j(\omega_{\mathrm{LD}} + n\omega_{\mathrm{RF}})t\big) \end{aligned} \tag{4}$$

Simply, considering to attain a high chirp factor [19]; many flat optical comb lines can be obtained by adjusting V_{RF1} and V_{RF2} values with slight voltage difference (small κ).

The simulated results that correspond to the indicated points (a) and (b) in Fig. 3 of the OFCS are shown in Fig. 4. The optical carrier launched into the DAM is shown in Fig. 4(a). Whereas, at the DAM output, broader and flattest quasi rectangular shape spectrum containing 47 useful frequency comb lines over frequency range observation of $192.8 - 193.4$ THz are obtained as depicted in Fig. 4(b). This outperforms the work conducted in [20] that achieved the same number of comb lines by applying a complex design using three cascaded external modulators. Based on that, and (4); it is clearly that the center frequency of the generated comb lines is determined by the center frequency f_{LD} of the CW laser diode (193.1 THz), while the comb lines spacing also called free spectral range (FSR) is governed by the frequency of the RF signal f_{RF} (12.5 GHz). Twenty (20) coherent flat optical carriers from 193.0125 (λ_1) to 193.25 (λ_{20}) THz are chosen as a proof-of-concept for the proposed system performance analysis in the downlink (DL)/uplink (UL) transmissions. The selected optical carriers in Fig. 4(b) are shown on the right side of Fig. 4. As we can see, the selected carriers have almost the same flatness could be identified by $f_n = f_{\mathrm{LD}} + nf_{\mathrm{RF}}$, where f_{LD} is the original frequency generated by the CW DFB-LD *ie* 193.1 THz,

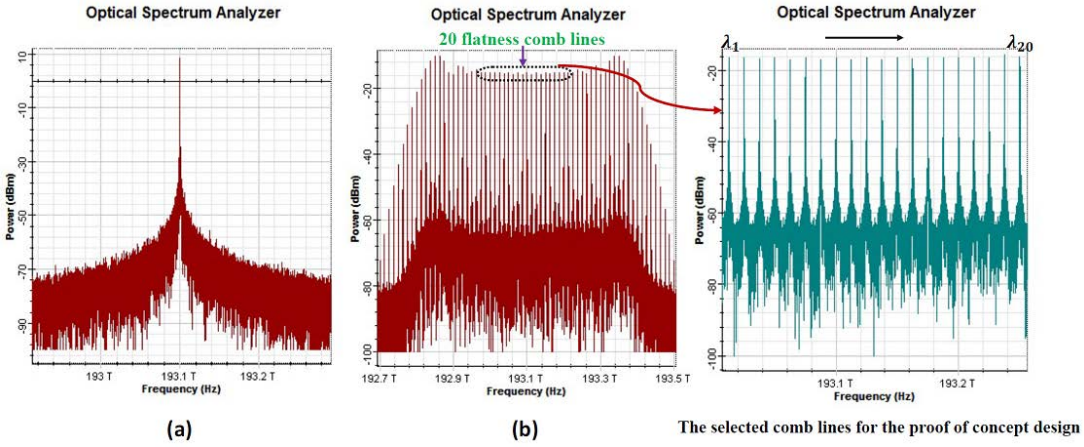

Fig. 4. (a) – Laser diode optical carrier, and (b) – the generated OFC lines

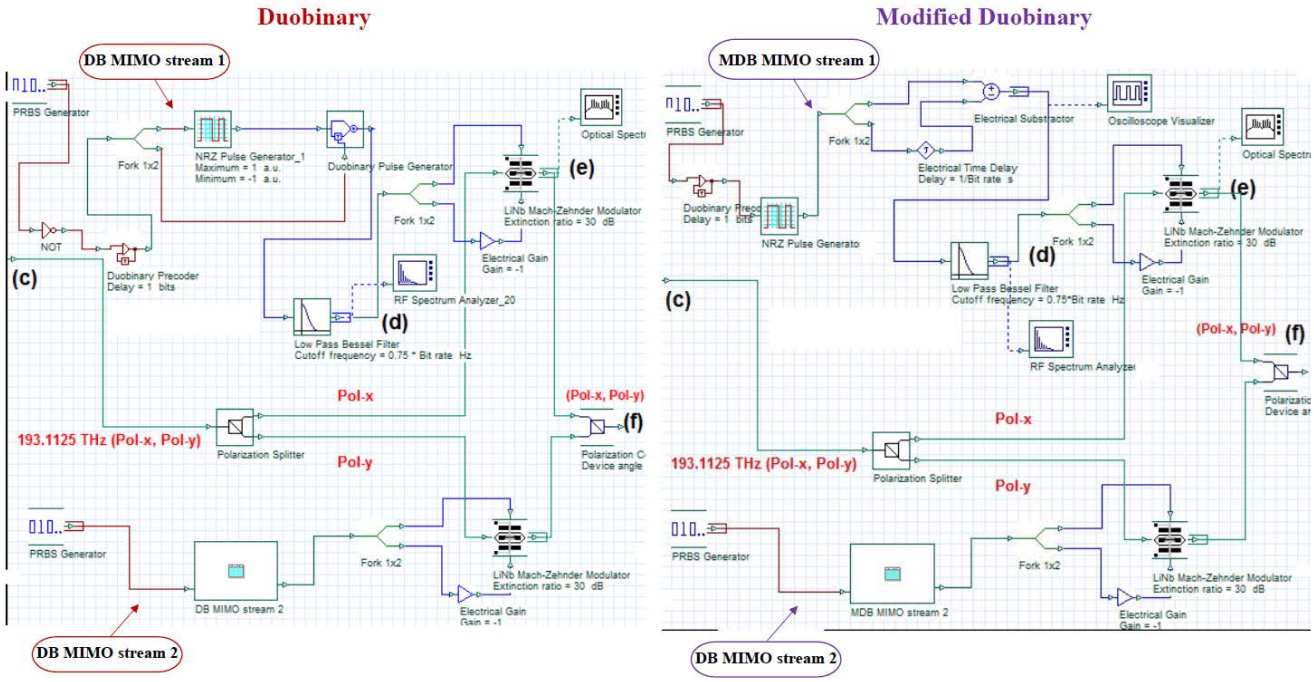

Fig. 5. The simulation setups of the DB and MDB modulations based PDM

f_{RF} is the RF source frequency (12.5 GHz), and n is the comb line index.

The number of wavelengths allocated in DL is equal to UL wavelengths. The optical sidebands marked by $\lambda_1, \lambda_2, \lambda_5, \lambda_6, \lambda_9, \lambda_{10}, \lambda_{13}, \lambda_{14}, \lambda_{17}$, and λ_{18}, are split into their x and y polarization components act as independent optical carriers to intensity modulate different broadband baseband duobinary (DB)/ modified duobinary (MDB) MIMO signals for the DL data transmission. Whereas, the unmodulated optical carriers denoted $\lambda_3, \lambda_4, \lambda_7, \lambda_8, \lambda_{11}$, $\lambda_{12}, \lambda_{15}, \lambda_{16}, \lambda_{19}$, and λ_{20} are delivered without imposing any data modulation to be used for mm-wave generation via RHD, and which are then used to transport time-multiplexed baseband DB/MDB MIMO signals for UL transmission.

For data modulation process, Fig. 5 shows the simulation setups of the binary data modulation through DB/MDB encoders and PDM. For electro-optical (E/O) conversion, the x-Pol and y-Pol components are applied to two parallel dual arm MZMs (DAM) for external intensity modulation by the MIMO stream 1 and MIMO stream 2 duobinary baseband signals. Therefore, the polarized-modulated data optical signals are subsequently multiplexed using a polarization beam combiner (PBC). As an example, the baseband DB/MDB MIMO streams 1 (d) are intensity modulated onto optical x-Pol

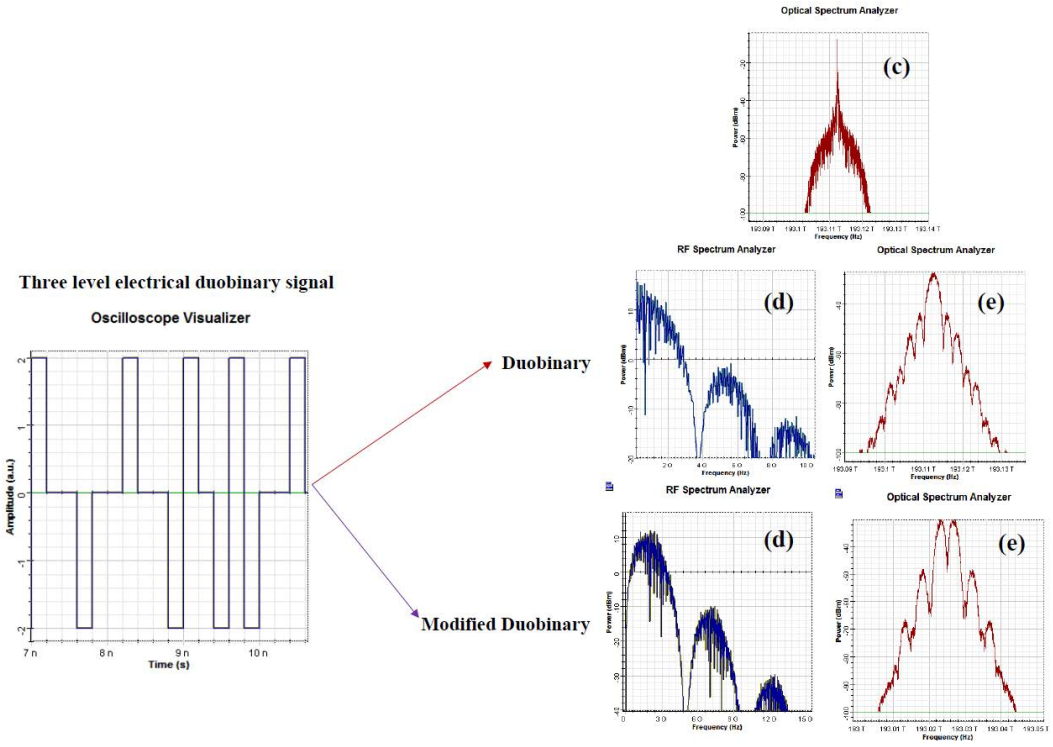

Fig. 6. RF and optical spectra analysis over the DB/MDB transmitters

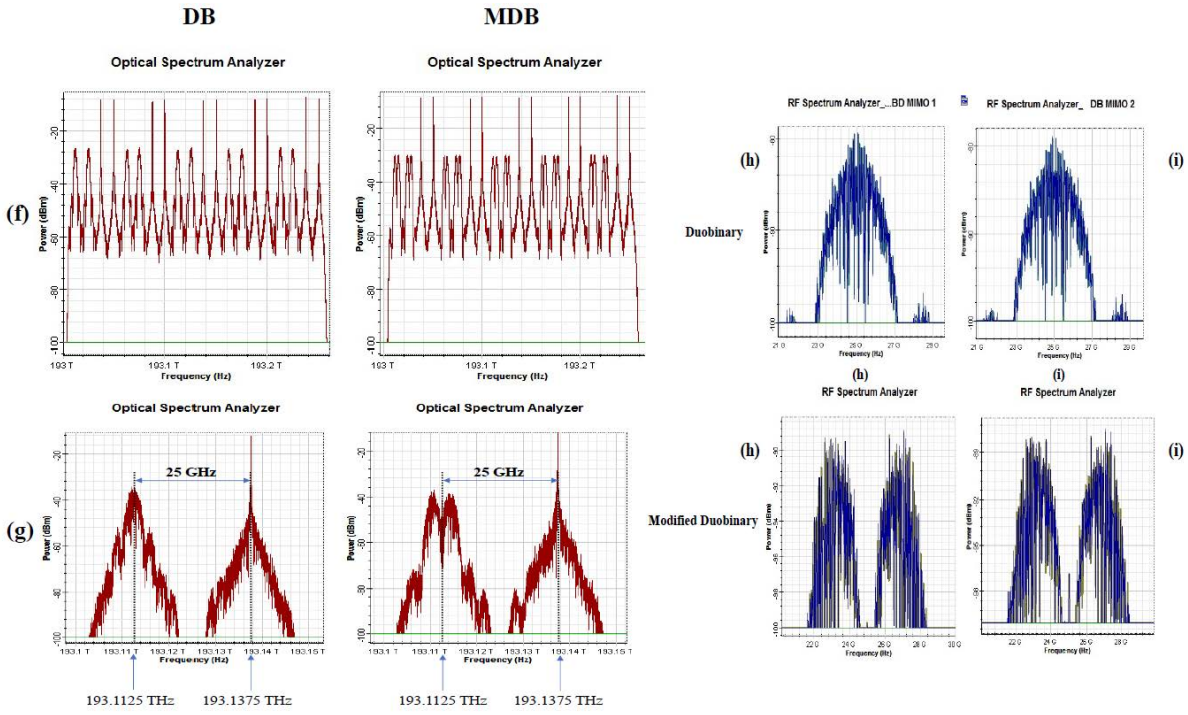

Fig. 7. The spectra tracing at various locations of the proposed ARoF-PON system over its downlink operation mode according to the indicated insets in Fig. 1(f) and Fig. 2(g,h,i) for DB and MDB.

state of the optical carrier (λ_9, 193.1125 THz) (c) via a DAM to produce the optical DB/MDB signals (e).

The three-level electrical duobinary signal and the aforementioned spectrums (c, d, e) according to the indicated insets in Fig. 5 are shown in Fig. 6 after the λ_9 channel filtering (x-pol). As Fig. 6(d) shows, the power of main lobe (useful data) is maximum in the electrical duobinary spectrum at zero frequency; and then tends to zero at its band edges. While it is zero in modified

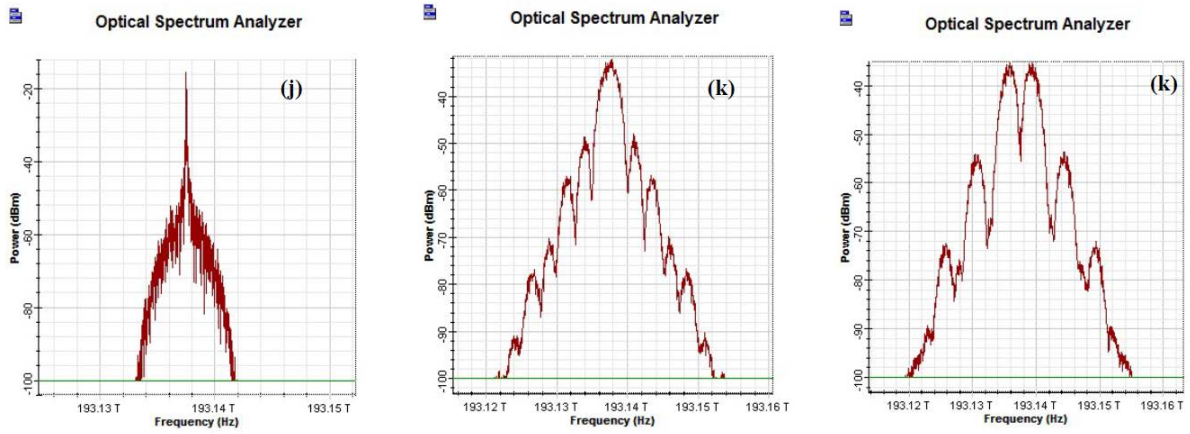

Fig. 8. Optical spectra according to the indicated insets in Fig. 2(j,k) for DB and MDB

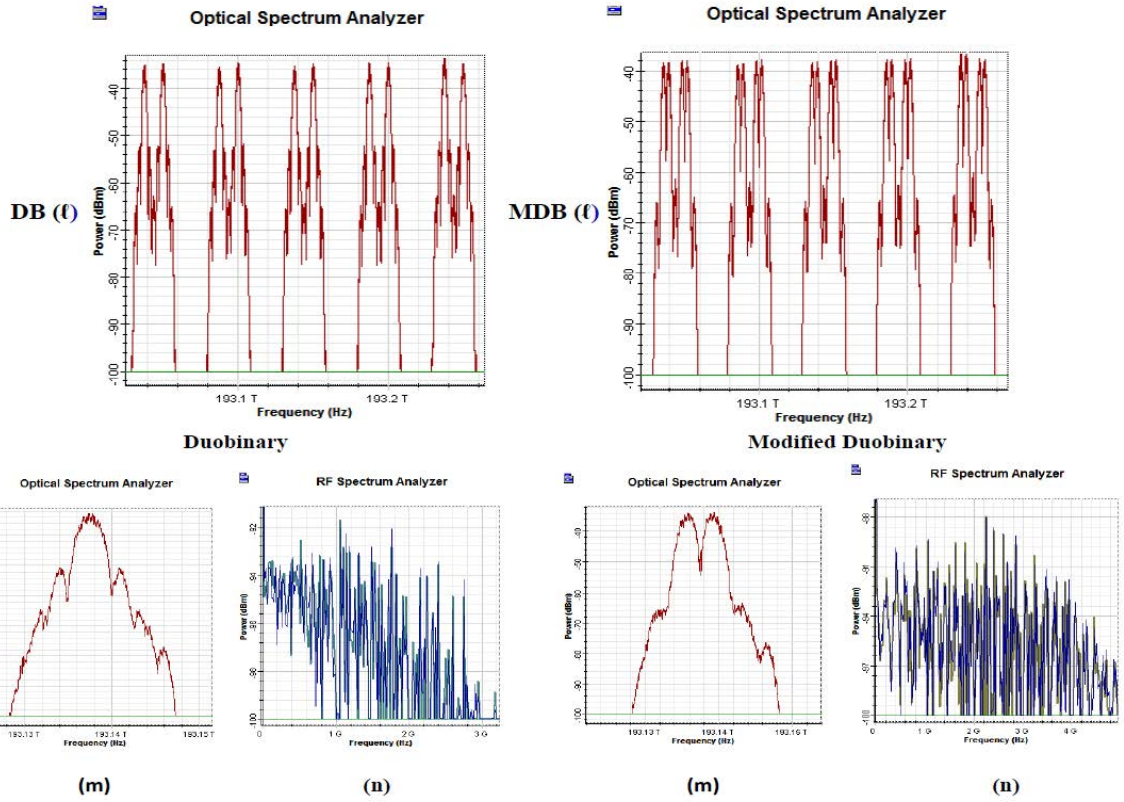

Fig. 9. The spectra tracing at various locations of the proposed ARoF-PON system over its uplink operation mode according to the indicated insets in Fig. 1(l,m,n) for DB and MDB

duobinary spectrum at zero frequency where concentrating most power of the main lobe around the zero.

The aforementioned modulated and unmodulated wavelengths are multiplexed using UDWDM-MUX, (f) in Fig. 1. In the spectrum plot in Fig. 7(f), the modulated optical carriers by DB or MDB are stacked, slightly broader in the spectrum, and have disparity in optical power compared to the unmodulated optical signals, and this implies the occurrence of insertion losses during modulation and multiplexing, see Tab. 1. At the RN, from the simulation fulfilment perspective; each pair of the polarization multiplexed signals as well as the unmodulated carriers spaced by the desired frequency are coupled with the help of optical couplers (OCs) acting as the role of the mm-wave allocator. In this work, a case study for 5G/5G+ scenario application working at 25 GHz k-band mm-wave frequency (3GPP n258 band) is adopted compliant with the blueSPACE project vision [21].

For RN-RAU spectrum analysis, two coupled optical carriers $(\lambda_9, \lambda_{11})$ ODN(B)as shown in Fig.1 have opted. It includes the modulated optical carrier (with DB or MDB) centered at 193.1125 THz, and unmodulated one at 193.1375 THz spaced apart from the former by a frequency spacing of 25 GHz. Figure 7(g) represents the optical spectrum of their x-pol signals at the upper photodiode (PD) after being polarized- demultiplexed at point (g) in Fig. 2. The modulated and unmodulated optical carriers are applied to the upper PD (or lower PD for y-

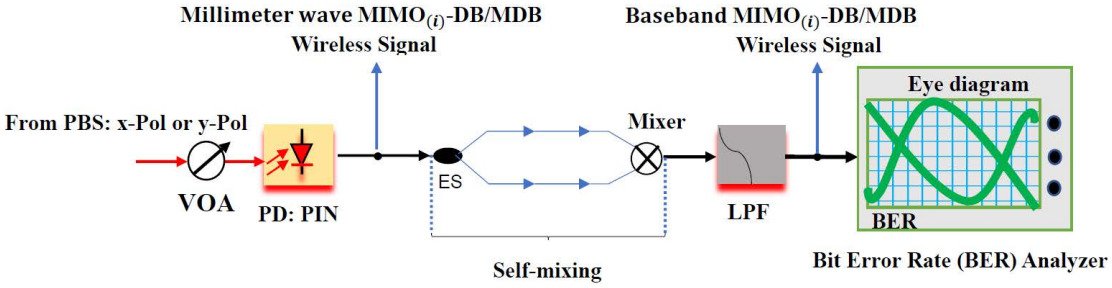

Fig. 10. The mm-wave down-conversion at the RAU used in the simulation

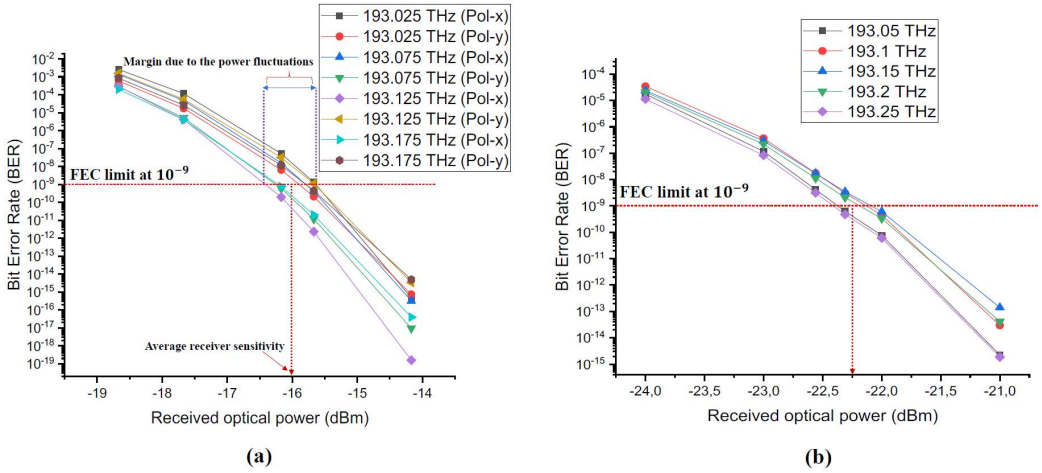

Fig. 11. BER versus ROP for DB of: (a) – DL, and (b) – UL

pol). Accordingly, at the PD output; DB and MDB signals exhibiting similar replica to the original baseband waveforms illustrated in Fig. 6 (d) are acquired. But they are transposed onto higher frequency band equivalent to the difference between the two coupled carriers (25 GHz) as depicted in the top and bottom at the right of Fig. 7(h,i), respectively. Noticeably, 2×2 MIMO modulated DB/MDB data signals at 25 GHz with high purity and stability, as compared to those depicted in Fig. 6(d), were successfully generated due to the realization of efficient beating between the two coherent optical carriers.

For the uplink transmissions, the time multiplexed baseband signal DB/MDB is modulated by a DAM onto the reserved blank optical carrier λ_{11} of 193.1375 THz filtered by the optical band pass filter (OBPF). The optical spectra are shown in Fig. 8(j,k). The modulated optical signals obtained from each RAU are then combined by UDWDM-MUX at RN to be transmitted towards the CO for UL transmission as Fig. 9(l) shown for DB and MDB, respectively. After UL data transmission, simple receivers using photodetectors followed by low pass filters are utilized. The received optical DB/MDB signals (193.1375 THz) at the UDWDM-DEMUX port output, Fig. 1(m), are depicted in Fig. 9(m). Whereas, the baseband photo-detected DB/MDB signals are observed in Fig. 9(n).

Notably, the simulated results in terms of spectral tracking are good consistent with theoretical analysis which proves the validity and applicability of the proposed system for practical usage. Moreover, all the key specifications of the used system components are summarized in Tab. 1. Furthermore, the major parameters adopted in the simulation model are matching to those used in the industry for on the field deployments in order to simulate the practical real environment to the fullest extent possible. It should be noted also that the optical amplifiers gain used at OLT for DL and UL were selected based on the simulation optimization process.

4 Results and discussion

4.1 Simulation setup configuration for transmission performance analysis

In this study, the wireless transmission is beyond the reach of interest. In order to emulate the receiving process of the MEU for analyzing the quality of the received signals in downlink, the generated mm-wave MIMO signals are directly down-converted at the RAU, where each demodulated signal is treated independently. For this purpose, we have utilized self-mixing technique similar to the used at the end mobile user terminal in RF domain to down-convert the electrical mm-wave wireless signal into baseband [15] as shown in Fig. 10. Once self-mixing is performed, a LPF is used for baseband signal pulse shaping in order to suppress the aliasing signals.

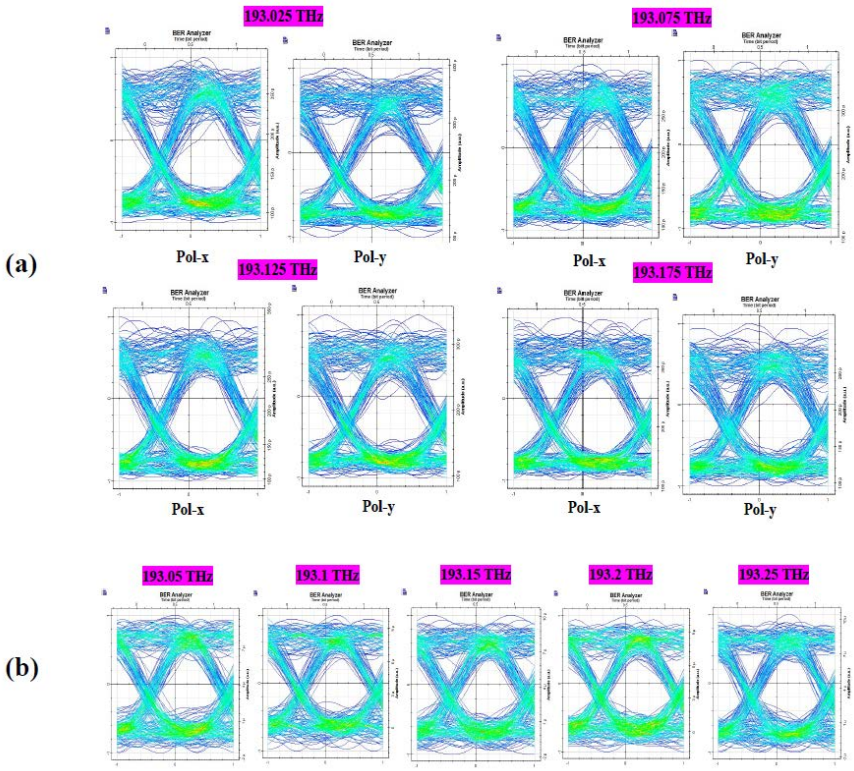

Fig. 12. The obtained DB eye diagrams of: (a) – DL, and (b) – UL

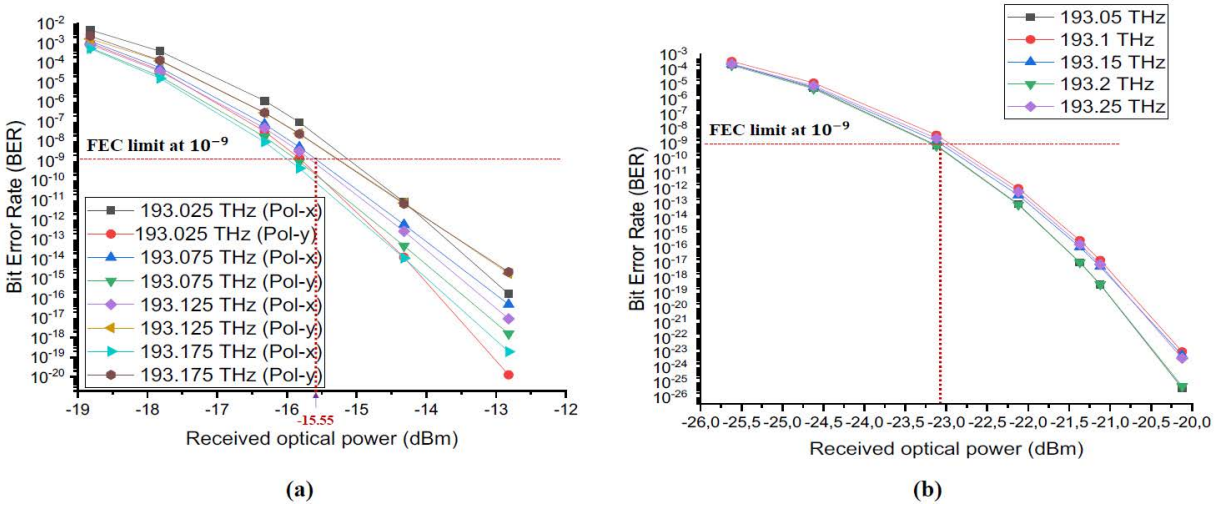

Fig. 13. BER versus ROP for MDB of: (a) – DL, and (b) – UL

It is worth to mention here that the downlink and uplink signals were transmitted over separated optical fiber links for the purpose to avoid the backscattering noise effect because the same unmodulated wavelengths in downlink are re-utilized for upstream data transmission (round-trip). In this context, the transmission performance of the proposed system is evaluated through bit error rate (BER) measurements for a given set of receiver sensitivities. It is conducted by varying the received optical power (ROP) with the aid of a variable optical attenuator (VOA) placed at the front of each photodetector as depicted also in Fig. 10. After recovering the baseband signals at the output of LPFs, are connected directly to the BER analyzers to estimate their BERs statistically from the correspond obtained eye diagrams, whereas, the received power is measured by using optical power meter.

4.2 The obtained results

In this work, for physical layer performance analysis simplicity; four polarized multiplexed random channels of 193.025, 193.075, 193.125, and 193.175 THz were chosen for downlink (DL). Whereas, five channels of 193.05, 193.1, 193.15, 193.2, and 193.25 THz for uplink (UL). In this regard, we have analyzed the transmission perfor-

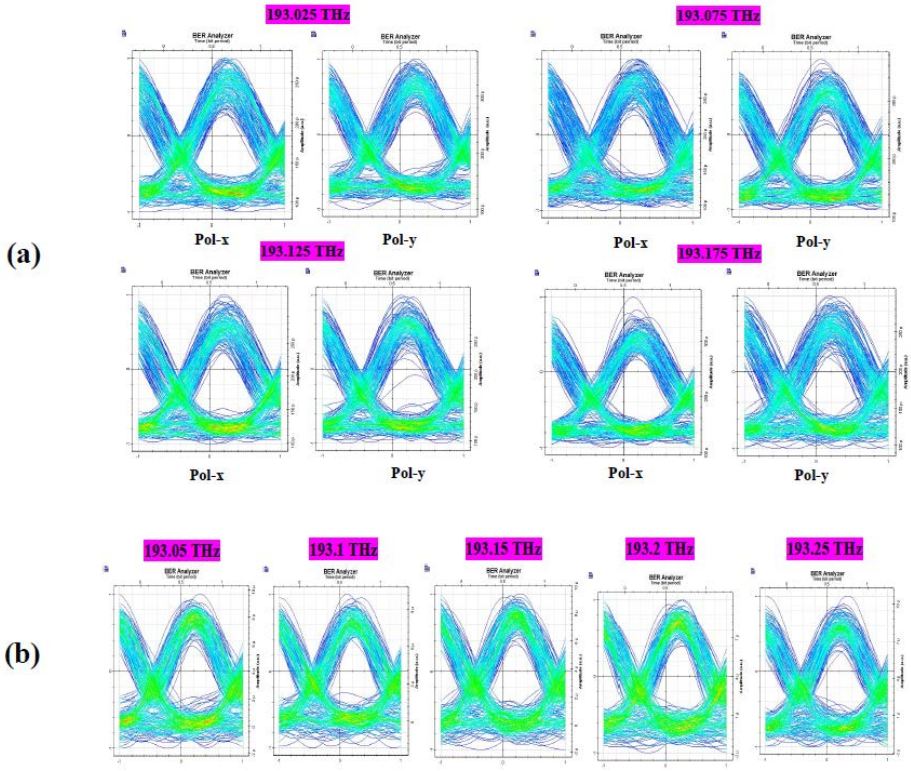

Fig. 14. The obtained MDB eye diagrams of: (a) – DL, and (b) – UL

mance with broadband data rate of 5 Gbps (per polarization in downlink) after 22 km full-duplex SMF transmissions.

4.2.1 DB transmission performance results

Figure 11 show the BER performance versus the ROP for duobinary (DB) at different RAUs and the OLT for DL and UL, after 22 km SMF transmissions.

In order to get further insight into the optical transmission characteristics, the eye diagrams of the received signals in the DL and UL directions at BER of $\approx 10^{-9)}$ after 22 km SMF are presented. The obtained eye diagrams of the down-converted DB mm-waves (DL) and directly detected optical DB signals (UL) are shown in Fig. 12.

4.2.2 MDB transmission performance results

Similar to the steps done for the DB mentioned earlier, BER is plotted as a function of the ROP for both directions. Therefore, Fig. 13 depicts the obtained results for MDB in DL and UL transmissions after 22 km SMF.

The transmission performance of MDB through eye diagrams that were retrieved at BER of $\approx 10^{-9}$ after 22 km SMF transmissions are also offered. The eye diagrams of the down-converted MDB mm-waves are shown in Fig. 14(a). Concurrently, for uplink, the obtained eye diagrams after direct detection of the optical MDB UL signals are presented in Fig. 14(b).

4.3 Discussion of the transmission performance results

Basically, the amount required optical received power to achieve certain BER threshold is named receiver sensitivity. Consequently, for transmission performance analysis the power receiver sensitivities are determined according to the BER curves. In this regard, the readings are taken at the BER of 10^{-9} which is defined as the forward error correction (FEC) limit reference for most optical communication system standards to offer an error-free transmission.

Depending on the above obtained BER results, the reason behind the fluctuations in received optical powers (ROPs) between the transmitted modulated data wavelengths in DL and UL is primarily due to the different propagation properties during the transmission over the optical fiber. Additionally, it is because the dissipation disparity in optical power caused by the optical components integrated across the different design levels. Moreover, the measured receiver sensitivities after 22 km SMF for all optical carriers at BER of 10^{-9} (margin band) are fluctuating from maximum to minimum. It is between -16.45 dBm to -15.65 dBm for DB and -16 dBm to -15.1 dBm for MDB in downlink. Whereas, it is from -22.4 dBm to -22.1 dBm for DB and -23.1 dBm to -22.9 dBm for MDB in uplink. As a result, error free transmissions at reasonable received optical powers were achieved. This is clearly indicating the power efficiency

Table 1. The ARoF-PON simulation model specifications

Component	Parameter
OFCS CW laser:	Frequency: 193.1 THz
	Optical power: 10 dBm
	Linewidth: 10 MHz
OFCS DAM:	Extinction ratio (ER): 30 dB
	Insertion loss: 3 dB
	Half-wave voltage V_π : 4 V
	Switching RF voltage: 4 V
	DC biases voltages V_{DC1}, V_{DC2} : 2 V
	Operation mode: asymmetric
	Electrical amplifiers Gain: 10 dB
Optical window:	C-band
OA:	Erbium-Doped Fiber Amplifier
	Operation mode: Gain control
	Gain: 10 dB
	Noise Figure (NF): 4 dB
UDWDM MUX/DEMUX (OLT, RN)	Bandwith: 10 GHz
	Channel spacing: 12.5 GHz
	(G.694.1 recommendation)
	Insertion loss: 3 dB
	Filter type: Gaussian
	Filter order: 2
PDM-DB/MDB (DL)/TDM -DB/MDB(UL) DAM:	Extinction ratio: 30 dB
	Half-wave voltage (V_π): 4 V
	Operation mode: Push-pull
	Insertion loss: 3 dB
OA (DL/UL)	Erbium-Doped Fiber Amplifier
	Operation mode: Gain control
	Gain: 12 dB (DL), 12 dB (UL)
	Noise Figure (NF): 4 dB

Component	Parameter
SMF (ODN)	Standard: ITU-T G.652
	Attenuation: 0.2 dB/km
	Dispersion coefficient: 16.75 ps/nm/km
	Dispersion slope: 0.075 ps/nm^2/km
	Differential group delay: 0.2 ps/km
	Polarization mode dispersion
	PMD coefficient: 0.05 ps/$\sqrt{\text{km}}$
	Self-phase modulation: enabled
	Length of feeder fiber: 20 km
	Length of distribution fibers: 2 km
Optical Couplers	Insertion loss: 2 dB
Micro-RAU Photodiodes (PDs):	Optical splitter, insertion loss: 2 dB
	Positive-Intrinsic-Negative (PIN)
	Responsivity: 0.9 A/W
	Dark current: 10 nA
	Self-mixing technique, electrical splitter insertion loss: 2 dB
	RF frequency carrier: 25 GHz
	(5G NR: k-band, 3GPP n258)
	MIMO streams: 2
Micro-RAU Optical band pass filter:	Center frequency: unmodulated optical carriers
	Filter type: Gaussian
	Filter order: 2
	Insertion loss: 3 dB
Low pass filters	Cutoff frequency: 0.75 × bit rate
	Filter type: Bessel
	Filter order: 4
	Insertion loss: 3 dB

of the proposed system in spite of no optical amplifiers or chromatic dispersion compensators in the ODN. Furthermore, from these different margins of receiver sensitivities (maximum to minimum) we can deduce that the power penalty is less than 1dB. Also, noteworthy that the downlink requires more receiving optical power than uplink. This due to the generation of modulated mm-wave signals through heterodyne detection that are then converted back into their original baseband formats by using self-mixing technique rather than simple direct detection that used for uplink.

According to the BER curves and above analysis; the average receiver sensitivities are measured by comparing DB and MDB for more precise investigations. In downlink, Fig. 11(a) and Fig. 13(a), the determined average receiver sensitivity of DB is -16.1 dBm, while it is around of -15.6 dBm for MDB. As a result, a power penalty of 0.5 dB was induced. It could imply that DB performance in terms of polarization mode dispersion (PMD) is slight superior compared to the MDB. Furthermore, this trend may be understood by the power penalties (less than 1 dB) that were observed between MIMO signals per each wavelength, which in turn could be attributed to the PMD effect and polarization dependent gain involved by the Erbium-Doped Fiber Amplifiers. In uplink, Fig. 11(b) and Fig. 13(b), the measured average receiver sensitivity for DB and MDB is about -22.3 dBm and *approx* $-$ 23.0 dBm, respectively, which leads to 0.7 dB in power penalty. It is evident that MDB is slightly better than DB. This could intuitively interpreted by the fact that the MDB has the highest tolerance to chromatic dispersion due to its narrow-bandwidth as compared to the DB. Moreover, this could attribute to the exceptional features of MDB in optical domain also called carrier-suppressed duobinary format, Fig. 6(e).

On the other hand, the gathered eye diagrams for both DB and MDB modulations in DL as well as UL are shown clearly with less noises. Apparently, all having the same degree of eye closure penalties with tiny differences. They also have maintained high-quality and quite good openings. This mainly could be explained upon, on one hand, to the low recorded power penalties < 1 dB thanks to the high tolerance property of DB/MDB modulations against chromatic and polarization mode dispersions. Furtherly, on the other hand, to the transport scheme used called baseband radio over fiber (BRoF) [22]. This approach could effectively mitigate the power fading induced by chromatic dispersion due to convey of baseband wireless signals over fiber in both directions instead of high frequency wireless ones. Accordingly, this is the main mo-

tivation behind using self-mixing technique at the RAU before doing optical intensity data modulation in uplink transmission (Fig. 2).

5 Conclusion

This paper addresses the proposition of a new cost-effective bidirectional ARoF transmission over UDWDM-PON intended for 5G/5G+ mm-wave wireless MIMO communication systems. A simple centralized optical comb technique with the incorporation of high spectral efficient duobinary modulations are adopted. The proposed system is able to deal with the generation of continuous tunable mm-waves by the allotment of coherent unmodulated carriers acting as beat sources for mm-wave generation. The unmodulated carriers are concurrently re-utilized also to offer colorless operation for uplink transmission (wavelength reuse) enabling free-laser base stations. The feasibility of the proposed fronthaul system has been successfully proven through the good conformability between the system spectra tracing and its relevant theoretical analysis counterpart. Furtherly, stable and high purity mm-wave DB/MDB MIMO signals ready for wireless transmission were obtained after RHD. According to the overall obtained results at a BER of 10^{-9} with respect to the used modulation schemes in terms of the measured and observed power penalties, no apparent receiver sensitivity degradations are caused, and the transmission performance does not render obvious tangible difference. It useful to conclude that hybrid DB/MDB for 5G mm-wave can be implemented for ubiquitous broadband connectivity. The proposed system can be viewed as an excellent solution to be part for long-term 5G and beyond (5GB) to fit the revolutionary demands of enhanced mobile broadband (eMBB) services with ultra-low latency data connectivity.

References

[1] "3GPP, User Equipment (UE) radio transmission and reception; Part 3: Range 1 and Range 2", *Interworking operation with other radios*, TS 38. 101-3 version 16. 0. 0 Release 16, 2019.

[2] G. Xiaohu, T. Song, M. Guoqiang, W. Cheng-Xiang, and H. Tao, "5G ultra-dense cellular networks", *IEEE Wireless Communications*, vol. 23, no. 1, pp. 72-79, 2016.

[3] I. Mehmet and B. Bostjan, "Proposal for distribution of a low-phase-noise oscillator signal in forthcoming fifth-generation mobile network by radio-over-fibre technology", *International Symposium ELMAR*, pp. 13-16, 2016.

[4] J. S.Saeed , H. Ashiq, Q. Muhammad Ali, and K. W. Shahid, "Towards the shifting of 5G front haul traffic on passive optical network", *Wireless Personal Communications*, vol. 112, no. 3, pp. 1549-1568, 2020.

[5] A. B. Dar, and F. Ahmad, "Optical millimeter-wave generation techniques: An overview", *Optik*, vol. 258, pp. 168858, 2022.

[6] K. Dimitrios, B. Thomas, R. Simon, J. Ulf, J. Martin, I. Marianna, S. Bart, and T. Idelfonso, "5G RAN architecture based on analog radio-over-fiber fronthaul over UDWDM-PON and phased array fed reflector antennas", *Optics Communications*, vol. 454, pp. 124464, 2020.

[7] K. Reinhard, C. Chrispine, and G. Tim, "Sub-60-GHz power- efficient fronthaul system of up to 16-Gbps using RF carriers generated from a gain-switched VCSEL", *OSA Continuum*, vol. 3, no. 12, pp. 3482-3496, 2020.

[8] S. Magidi, and A. Jabeena, "Bidirectional MDRZ downstream and NRZ OOK upstream SS-WDM RoFSO communication system", *Journal of Optical Communications*, 2019.

[9] G. Aamir, and G. Salman, "Self-phase modulation-based multiple carrier generation for radio over fiber duplex baseband communication", *Photonic Network Communications*, vol. 29, no. 2, pp. 133-137, 2015.

[10] B. Aziz, T. Mehmood, and S. Ghafoor, "UWB over fiber transmission to multiple radio access units using all-optical signal processing", *Photonic Network Communications*, vol. 34, no. 2, pp. 280-287, 2017.

[11] T. Mehmood, and S. Ghafoor, "Millimeterwave signal generation and transmission to multiple radio access units by employing nonlinearity of the optical link", *International Journal of Communication Systems*, vol. 32, no. 1, pp. 1-11, 2019.

[12] L. Sharan, G. Shanbhag, and K. Chaubey, "Design and simulation of modified duobinary modulated 40 Gbps 32 channel DWDM optical link for improved non-linear performance", *Cogent Engineering*, vol. 3, no. 1, 2016.

[13] M. H. Ullah, M. Tareq , H. Ashiq , A. Moustafa, and M. Sanaullah, "FWM reduction using different modulation techniques and optical filters in DWDM optical communication systems: a comparative study", *Iranian Journal of Science and Technology, Transactions of Electrical Engineering*, vol. 43, no. 3, pp. 479-488, 2019.

[14] D. Nguyen, and M. Amin, "Transmission of Duobinary Signal in Optical 40 GHz Millimeter-Wave Radio-Over-Fiber Systems Utilizing Dual-Arm LiNbO3 Mach-Zehnder Modulator for Downstream", *Journal of Optical Communications*, vol. 37, no. 2, pp. 155-161, 2016.

[15] L. Cheng, C. Hung-Chang, F. Shu-Hao, H. Yu-Ting, L. Jie, Z. Liang, Y. Jianjun, and C. Gee-Kung, "A novel self-mixing duobinary RF receiver for millimeter-wave radio-over-fiber systems", *Optical Fiber Communication Conference*, Optical Society of America, 2012.

[16] H. Chien, C. Arshad, and C. Gee-Kung, "Systems and methods for providing an optical information transmission system", *U.S. Patent* Application No. 13/035,827.

[17] A. Ahmad, D. Choi, and S. Ullah, "A compact two elements MIMO antenna for 5G communication", *Scientific Reports*, vol. 12, no. 1, pp. 1-8, 2022.

[18] H. Yousif, and M. Tahreer, "Relationship between the voltage applied to MZM arms and the generation of optical frequency comb", *International Journal of Engineering & Technology*, vol. 7, no. 415, pp. 405-408, 2018.

[19] H. Jassim, E. Siamak, N. Kamarul, A. Harith, H. Sulaiman, and S. Hossam, "Optical frequency comb generation based on chirping of Mach-Zehnder modulators", *Optics Communications*, 344, pp. 139-146, 2015.

[20] Z. Chan, N. Ti-Gang, L. Jing, P. Li, L. Chao, and M. Shaoshuo, "A full-duplex WDM-RoF system based on tunable optical frequency comb generator", *Optics Communications*, vol. 344, pp. 65-70, 2015.

[21] R. Thiago, R. Simon, T. Idelfonso, V. Chris, K. George, and P. Nikos, "Analog radio-over-Fiber 5G fronthaul systems: blueSPACE and 5G-PHOS projects convergence", *European Conference on Networks and Communications (EuCNC*,)pp. 479-484, 2019.

[22] S. Redhwan, A. Mohammad, A. Abdulaziz, and A. Samir, "Wireless signals transport schemes in fiber wireless systems", *IEEE 4th International Conference on Photonics* (ICP), pp. 47-49, 2013.

Received 24 January 2023